CFD-modelling of natural convection in a groundwater-filled borehole heat exchanger

A-M. Gustafsson, L. Westerlund, G. Hellström

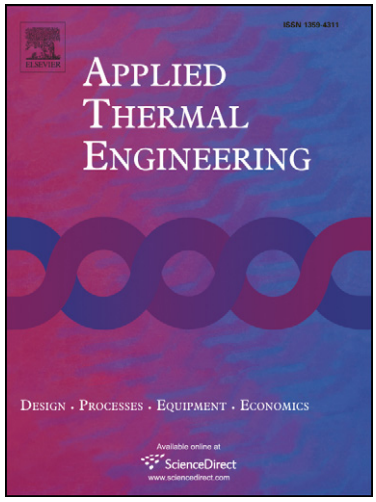

CFD-modelling of natural convection in a groundwater-filled borehole heat exchanger

A-M. Gustafsson, L. Westerlund, G. Hellström

PII: S1359-4311(09)00344-5
DOI: 10.1016/j.applthermaleng.2009.11.016
Reference: ATE 2934

To appear in: *Applied Thermal Engineering*

Received Date: 6 March 2008
Accepted Date: 20 November 2009

Please cite this article as: A-M. Gustafsson, L. Westerlund, G. Hellström, CFD-modelling of natural convection in a groundwater-filled borehole heat exchanger, *Applied Thermal Engineering* (2009), doi: 10.1016/j.applthermaleng.2009.11.016

CFD-modelling of natural convection in a groundwater-filled borehole heat exchanger

(CFD-modelling of a water-filled BHE)

A-M. Gustafsson[a*], L. Westerlund[b] G., Hellström[c]

[a] Department of Civil, Mining and Environmental Engineering, Luleå University of Technology, SE-971 87 Luleå, Sweden

[b] Department of Applied Physics and Mechanical Engineering, Luleå University of technology, SE-971 87 Luleå, Sweden

[c] Physics, Lund University, Box 118, SE-221 00 Lund, Sweden

*Corresponding author. Address: Luleå University of Technology, SE-971 87 Luleå, Sweden. Tel: +46 920 49 23 08. Fax: +46 920 49 16 97. E-mail: amg@ltu.se

Abstract

In design of ground-source energy systems the thermal erformance of the borehole heat exchangers is important. In Scandinavia, boreholes are usually not grouted but left with groundwater to fill the space between heat exchanger pipes and borehole wall. The common U-pipe arrangement in a groundwater-filled BHE has been studied by a three-dimensional, steady-state CFD model. The model consists of a three meter long borehole containing a single U-pipe with surrounding bedrock. A constant temperature is imposed on the U-pipe wall and the outer bedrock wall is held at a lower constant temperature. The occurring temperature gradient induces a velocity flow in the groundwater-filled borehole due to density differences. This increases the heat transfer compared to stagnant water. The numerical model agrees well with theoretical studies and laboratory experiments. The result shows that the induced natural convective heat flow significantly decreases the thermal resistance in the borehole. The density gradient in the borehole is a result of the heat transfer rate and the mean temperature level in the borehole water. Therefore in calculations of the thermal resistance in groundwater filled boreholes convective heat flow should be included and the actual injection heat transfer rate and mean borehole temperature should be considered.

Keywords: Natural convection, borehole heat exchanger, buoyant flow, numerical model, groundwater filled borehole, U-pipe

Nomenclature

A	Aspect ratio = $L/(r_{bhw}-r_{po})$
c_p	Specific heat (J/kg,K)
g	Acceleration due to gravity (m/s^2)
E	Experiment
f	Fanning friction factor
h	Convective heat transfer coefficient (W/m^2,K)
L	Borehole length (m)
$\dot{m}$	Mass flow rate (kg/s)
M	Model
N_{hf}	Heat flux number = q''_{bhw}/q''_{po}
Nu	Nusselt number
Nu*	Estimated Nusselt number = $R^*_{w,c}/R^*_{w,t}$
Pr	Prandtl number
q'	Heat flow (W/m)
q"	Heat flux (W/m^2)
r	Radius (m)
R	Radius ratio = r_{bhw}/r_{po}
Ra*	Modified Rayleigh number = $g\beta q''_{po}\left(r_{bhw}-r_{po}\right)^4/\lambda\nu\alpha$
R_b	Borehole thermal resistance (K,m/W)

R_w Thermal resistance in borehole water, between outer pipe wall and borehole wall (K,m/W)

Re_D Reynold number = $4\dot{m}/2\pi \cdot r\mu$

T Temperature (ºC or K)

Greek symbols

α Thermal diffusivity = $\lambda / (\rho \cdot c_p)$ (m^2/s)

β Thermal expansion coefficient (1/K)

λ Thermal conductivity (W/m,K)

ν Kinematic viscosity (m^2/s)

μ Dynamic viscosity (kg/s,m)

ρ Density (kg/m^3)

Δ Difference/gradient

Subscripts

a Annulus

bhw Borehole wall

br Bedrock

brb Outer vertical bedrock boundary

c Conductive heat transfer

f Heat carrier fluid

p Pipe

pi Inside of pipe wall

po Outside of pipe wall

ref	Reference
t	Total
u	U-pipe

1. Introduction

Borehole heat exchanger (BHE) systems use the ground as a heat source or sink for space conditioning in residential and commercial buildings. In Scandinavia groundwater is often used to fill the space between borehole wall and collector wall, while otherwise it is more common to backfill with some grouting material. The advantage of using water is cheaper installations and more easy access to the collector if needed. Grouting is on the other hand required in many counties by national legislation in order to prevent groundwater contamination or is used to stabilize the borehole wall. In Sweden the most common bedrock is crystalline granite with few fractures, as a result the use of groundwater filled boreholes is dominant.

This paper covers heat injection in a groundwater-filled BHE with a single U-pipe collector. During operation of the system a temperature gradient is developed in and around the borehole. When the temperature changes in the water a volume expansion or reduction is induced, resulting in changes in the density. Dense water will start to sink and less dense water to rise. The induced natural convective flow will result in a better heat transfer through the borehole water. It will depend on the mean temperature level in the borehole water and injection heat transfer rate the system is working with.

Most BHE calculation models are 1D or 2D using only conductive heat transfer [1, 2]. The thermal process is usually divided into two separate regions, the solid bedrock outside the borehole and the region inside the borehole. Since the aspect ratio is quite small, transient

heat transfer in the bedrock is often modelled according to the 1D line-source or the cylindrical-source theory. Regarding long-term responses for the BHE, the dynamic temperature changes inside the borehole are small compared to those in the ground. Therefore, the thermal process inside the borehole is commonly treated as steady-state heat transfer and described by a constant borehole thermal resistance, R_b [K,m/W]. This includes heat transfer from the bulk heat carrier fluid through both the collector pipe and the filling material in the borehole.

Few models concern the convective heat transfer in the groundwater. Most of them are dealing with regional groundwater flow [e.g. 3, 4], which is shown not to influence the system except in porous ground or high fractured bedrock. Other studies have shown that during certain conditions regional groundwater flow may increase the heat transfer even for small Darcy flows [5, 6]. There is also a study on thermosiphon effects where groundwater filled borehole in fractured rock experiences a convective flow through the borehole into connecting fractures, increasing the heat transfer in the bedrock as well as the borehole [7]. None of these models concern natural convection in groundwater filled borehole situated in solid rock without any larger fractures, which is a common situation in Sweden.

Water has a thermal conductivity of approximately 0.6 W/m,K, which would result in a rather high borehole thermal resistance, R_b~0.15 to 0.2 K,m/W (including heat transfer through the U-pipe and circulating fluid) in a common single U-pipe borehole heat exchanger. However, the induced convection increases the heat transfer and most measurements in the groundwater-filled single U-pipe BHE result in a borehole thermal

resistance R_b~0.06 to 0.08 K,m/W during heat injection. A larger borehole thermal resistance results in a larger temperature difference between the borehole wall and mean fluid temperature. For a certain undisturbed ground temperature and a specific heat injection rate a larger R_b will result in a higher fluid temperature up to the heat pump. For a heat pump injecting heat a high return temperature from the ground decrease the performance of the heat pump resulting in a higher electricity demand. It is therefore always desirably to have as low thermal resistance in the borehole and ground as possible.

As mentioned, the temperature-dependent natural convection in the groundwater is not modelled in current simulation tools and commercial software for BHE systems. Instead the borehole's thermal resistance is usually measured during a thermal response test (TRT) for a certain heat transfer rate injection or an assumed representative value for the given loading conditions is used. Thermal response tests are performed during approximately 72 hours in Sweden, after it is assumed to be steady-state conditions.

During a year of operation the heat transfer rate achieved and the temperatures received by the system differs depending on the season. The convective heat transfer will therefore change during the year which will result in different borehole thermal resistances. This study concerns the influence of natural convection on the borehole's thermal resistance for different heat transfer rates and temperature levels in solid bedrock without fractures. The results from the model are compared to other published numerical model and laboratory experiments.

2. Simulation models

Two different 3D, steady-state models were built and simulated in the CFD-software Fluent. The software uses a finite volume method to convert the governing equations to numerically solvable algebraic equations [8]. A commonly investigated convection model in the literature is the annulus model. Such model (M_a) was constructed (Fig. 1a) to compare the result with published experimental result and numerical simulation, described in section 3. The second model (M_u) is a section of a U-pipe in a groundwater-filled borehole with surrounding rock (Fig. 1b). This model is used to investigate how the borehole thermal resistance (R_b) is affected by the convective flow. Of interest is how the R_b change for different temperature conditions in the borehole water and heat transfer rates. It is also compared with experimental results, section 4.

The annulus model (M_a) consists of two 1 m long cylinders with water filling the space between them (Fig. 1a). The outer radius was set to the same value as the borehole radius (r_{bhw}) and the inner radius (r_{po}) was chosen so that the conditions were similar to these in the published papers [9, 10]. The numerical mesh consists of a total of 91000 cells of hexahedron and wedge-shaped volume elements in the borehole. A constant heat flux is given at the inner cylinder (q''_{po}) and a constant temperature at the outer cylinder (T_{bhw}). The bottom and top boundaries are treated as adiabatic surfaces.

The U-pipe model (M_u) consists of a 3 m long and vertical groundwater-filled borehole containing a single U-pipe collector (Fig. 1b). The cylindrical region outside the borehole

consists of solid bedrock with material parameters similar to granite (ρ_{br}=2360 kg/m^3; $c_{p,br}$=775 J/kg,K; λ_{br}= 3 W/m,K) extending to a radius of 1 m. Due to the U-pipe configurations, the heat flow close to the pipes will not be radial. The volume between the borehole wall and the U-pipe is water-filled with material parameters according to Table 1. All the material parameters except the density are kept constant for each simulation. In this model a constant temperature is set at the outside of the pipe wall (T_{po}) which should be an acceptable approximation for a 3 m long borehole at steady-state conditions. For the other boundary conditions, the outer vertical bedrock boundary is set to a constant temperature (T_{brb}) and the bottom and top boundaries are treated as adiabatic surfaces.

The numerical mesh consists of hexahedron and wedge-shaped volume elements, in total about 634000 cells. For both models refining the mesh within the possibilities of the computer strength render changes <<1%. The mesh has been checked for cell skewness and aspect ratio according to normal CFD standard. During the simulations all residuals were run down to $<5\cdot10^{-5}$. Using conductive heat flow through the water and the bedrock the model has been compared to an analytical exact model [11] and the difference in result were <1%. The validation of the convective heat flow through the borehole water is presented for an annulus geometry in section 3. Figure 2 shows the mesh in a cross-section of the borehole and part of the bedrock.

In Fluent and for natural convection heat flows the Boussinesq approximation can be used to describe the fluid density as a function of temperature. The model treats density as a constant value in all solved equations, except for the buoyancy term in the momentum

equation. It is valid for $\beta(T - T_{ref}) << 1$ which is true for the temperature gradients in the borehole water. The buoyancy term in the momentum equation is then approximated to Eq. (1).

$$(\rho - \rho_{ref})g \approx -\rho_{ref}\beta(T - T_{ref})g. \quad (1)$$

The densities versus temperature curve for water is non-linear (Fig. 3) with highest density value for a temperature level of approximately 4ºC [12]. The non-linearity will affect the occurring density differences at a certain mean temperature level in the borehole water. Lower mean temperature levels will result in smaller density differences for the same temperature gradient between pipe wall and borehole wall. If the mean temperature level in the borehole water is 10ºC, a temperature gradient of 1ºC will result in a density difference of 0.08 kg/m^3. While at a mean temperature of 25ºC in the borehole water a temperature gradient of 1ºC result in 0.25 kg/m^3 in density difference. These differences in density will result in an increased velocity for the higher temperature level. Other parameter values for water (for instance kinematic viscosity) vary in the same direction and magnify the process. Thus there will be a decrease in borehole thermal resistance for increased borehole mean temperature.

3. Validation of numerical model

In 1983, Keyhani et al. [9] investigated free convection in a vertical annulus. They used an annulus-shaped experimental configuration with radius ratio R=4.33 and aspect ratio A=27.6, i.e. the effective heated length was 87.6 cm, the inner diameter was 1.91 cm and the outer diameter was 8.26 cm. The boundaries had constant heat fluxes over the inner radius and isothermal conditions on the outer radius. Two gases were used, air (Pr = 0.71 at 300 K) and helium (Pr = 0.68 at 300 K). The experimental results were fitted with a power-law dependence of aspect and radius ratios, and gave the following Nusselt number correlation, Eq. (2).

$$Nu = 0.291 \cdot \left(Ra*\right)^{0.244} A^{-0.238} R^{0.442}, \quad 1.8 \cdot 10^4 \le Ra* \le 4.21 \cdot 10^7. \tag{2}$$

In 1986, Littlefield and Desai [10] examined buoyant laminar convection in a vertical cylindrical annulus. The numerical model had a constant heat flux on the inner radius and either isothermal conditions or constant heat flux on the outer radius. The model was valid for Pr=10. They suggested the following relationship of Nusselt's number for isothermal boundary condition, Eq. (3).

$$Nu = 0.443 \cdot A^{-0.245} R^{0.44} \left(Ra*\right)^{(0.233-0.009R)}, \ 1.5 \le R \le 5, 10 \le A \le 50, \left|N_{hf}\right| \le 0.5, \text{and } Ra* \le 10^8 \tag{3}$$

An annulus model, M_a, was assembled with measures according to Fig. 1a, giving the aspect ratio A=31.45 and radius ratio R=2.59. The inner surface was given a constant heat flux and the outer surface a constant temperature. The annulus was filled with water

reaching a temperature of 281 K, giving a Prandtl number of 9.97. The model was built to match the conditions of Littlefield and Desai's numerical model and also the outer radius was chosen to be the same as the borehole radius in the U-pipe model (M_u), r_{bhw}=0.0518 m. Steady-state models require the same heat flow rate per meter in length (q') over both inner and outer surfaces, according to energy balance. The inner radius was chosen to satisfy the condition $\left|N_{hf}\right| = 0.386 \leq 0.5$, whereby r_{po}=0.02 m.

Five different heat flow rates were used (25, 50, 75, 100 and 125 W/m) on the inner radius (r_{po}) in the simulations. At the outer boundary, temperatures were held constant at 280 K. The estimated Nusselt number, Nu^*, was calculated, Eq. (4), as a quota between the thermal resistance with pure conductive heat transfer in the borehole water ($R_{w,c}$) and the thermal resistances in the borehole water for the actual or total heat transfer including the convection ($R_{w,t}$) [14].

$$Nu^* = R_{w,c} / R_{w,t} \tag{4}$$

The thermal resistance in the borehole water for conductive heat transfer ($R_{w,c}$) is calculated as conductive heat transfer in one dimension for an annulus, Eq. (5).

$$R_{w,c} = \frac{\ln\left(r_{bhw}/r_{po}\right)}{2\pi\lambda} \tag{5}$$

The total resistance in the borehole water ($R_{w.t}$) is calculated from the simulation result, according to Eq. (6). The temperatures are calculated as surface mean values and the heat flow is given per meter of borehole length.

$$R_{w,t} = \frac{T_{bhw} - T_{po}}{q'} \tag{6}$$

In Fig. 4, Nusselt number correlations according to Eq. (2), (3) and (4) are shown as a function of the modified Rayleigh number. Ra* has been calculated with the material parameters for water for the actual mean temperature and with the heat transfer flux from the calculations. The agreement between the Fluent validation model and the reference Nusselt correlations is good, especially in relation to Littlefield and Desai's numerical model.

4. Comparison with laboratory measurement on a U-pipe borehole

In 1999, Kjellsson and Hellström [15, 16] conducted a laboratory study of heat transfer in a water-filled borehole with different collector arrangements. The test equipment consisted of an outer 3 m high steel cylinder with a diameter of 0.4 m. A cryostat-controlled circulating fluid maintained the cylinder at a certain temperature (T_{brb}). An inner, concentric plastic pipe with an inner diameter of 0.1036 m represented the borehole wall. The annular ground region between the borehole and the steel cylinder was filled with a mixture of fine sand

and a water-antifreeze fluid. Several collector types were tested. The tests were run at least three days and steady-state conditions were attained after about one day.

The single U-pipe DN40PN6 measurements from their experiment are here compared to the Fluent U-pipe model (M_u) described in Section 2 and Fig. 1b. The test was performed for different cryostat temperatures and heat injections rates. To minimize influence of heat losses to the surroundings, the injection rate for each measurement was calculated from the temperature gradient over the ground region assuming only conductive heat transfer and constant conductivity. Table 1 shows the cryostat temperature, here named T_{brb}, and injection rate for each experimental measurement, named E1-E12.

Boundary conditions in the model were given as a constant temperature at the outer bedrock boundary (T_{brb}) and a constant temperature at the U-pipe outer wall (T_{po}). Water physical properties were taken from standard water parameter table [12, 13] for the same temperature as the reference temperature (T_{ref}) in the Boussinesq equation. T_{ref} was chosen to be a half degree less than the wall temperature (T_{po}) and thereby close to the mean borehole temperature. In Table 1, model boundary conditions and reference parameters are presented for the different simulations, named M_u1-M_u6.

4.1 Heat transfer through U-pipe wall and heat carrier fluid

The heat transfer through the collector pipes and the fluid inside must be added to the numerical model to be able to compare with the experimental results. The DN40PN6 U-pipe has an outer radius of 0.02 m and an inner radius of 0.0177 m (Fig. 5).

The thermal conductivity for the pipe is assumed constant over the temperature interval, λ_p = 0.42 W/m,K. The temperature on the inside of the pipe (T_{pi}) is calculated according to Eq. (7), where the temperature on the outside of the pipe wall (T_{po}) and the heat transfer rate (q') is received from the numerical simulation.

$$T_{pi} = q' \cdot \frac{\ln\left(r_{po}/r_{pi}\right)}{2\pi\lambda_p} + T_{po} \tag{7}$$

To calculate the mean fluid temperature the heat transfer through the fluid has to be established. The convective heat transfer coefficient in the fluid is calculated by using Eq. (8-11) [14]. The volume flow rate is set to 0.97 l/s, the same as in the experiment [15, 16]

$$\mathrm{Re}_D = \frac{4\dot{m}}{2\pi\mu \cdot r_{pi}} \tag{8}$$

$$\mathrm{f} = \left(1.58 \cdot \ln\left(\mathrm{Re}_D\right) - 3.28\right)^{-2} \tag{9}$$

$$Nu = \frac{\left(\mathrm{f}/2\right) \cdot \left(\mathrm{Re}_D - 1000\right) \cdot \mathrm{Pr}_f}{1 + 12.7\sqrt{\mathrm{f}/2} \cdot \left(\mathrm{Pr}_f^{2/3} - 1\right)} \tag{10}$$

$$h_f = \frac{Nu \cdot \lambda_f}{2 \cdot r_{pi}} \tag{11}$$

The mean fluid temperature (T_f) may now be calculated according to Eq. (12)

$$T_f = \frac{q'}{h_f 2\pi \cdot r_{pi}} + T_{pi} \tag{12}$$

The borehole thermal resistance (R_b) is calculated as the temperature difference between mean fluid temperature (T_f) and borehole wall temperature (T_{bhw}) divided by the heat transfer rate (q') Eq. (13). Notice, in the experiment T_f is the mean value of the ingoing and outgoing flow while for the model T_f is calculated according to Eq. (12). The mean fluid temperature in the model is calculated from the mean value of the outer pipe temperature, T_{po}. This may introduce some error in the comparison but for a three meter long borehole this ought to be insignificant.

$$R_b = \frac{T_f - T_{bhw}}{q'} \tag{13}$$

5. Results

Borehole thermal resistances from experiment and the numerical model (Eq. 13) are shown in Fig. 6 as a function of fluid temperature. They show a decreased value for increased fluid temperatures, which is a result of a larger convective heat flow. The velocity flow is determined of the density differences in the borehole water. As discussed earlier, there will be an increased density difference for an increased mean temperature level (in the temperature interval of interest, 10-35ºC) due to the non-linearity of the density-temperature curve. A larger density difference in the borehole water results in higher flow velocities and thus a more effective heat transfer. The model shows in general higher values, up to around 14 % higher compared to the experimental results.

In Fig. 6 for a mean fluid temperature of 23-24ºC there are two different borehole thermal resistances. The higher value is from simulation M_u2 with 55 W/m heat injection rate and the lower from M_u5 with 101 W/m. The almost twice as high heat injection rate in simulation M_u5 results in a decrease in borehole thermal resistance of 2.6%. The same may also be seen around 32-33ºC where the thermal resistances for M_u3 (50 W/m) and M_u6 (95 W/m) differs with 3%. The same percent is achieved between M_u2 and M_u3 where the heat injection rates are almost the same but the mean temperatures differ with 8ºC.

Due to the U-pipe configuration the heat flow close to the pipes will not be radial. After a short distance the heat flow will be more evenly distributed and a radial pattern will take form at a certain distance from the borehole. In Fig. 7a temperatures in and around the borehole are shown. The un-radial shape is clearly visible inside the borehole water, while a

radial pattern is seen shortly after entering the bedrock. In Fig. 7b temperatures are shown along the borehole wall in the length direction. The highest temperatures are obtained in the x-direction where the U-pipe is close to the borehole wall and the lowest in the z-direction. The borehole thermal resistance calculated from the model uses an area averaged mean value for all its parameters.

These differences in temperature at the borehole wall will affect the heat transfer in the bedrock close to the borehole. Figure 8 shows the temperature difference between the x and z-direction in the bedrock at the vertical level 1.5 m for simulations M_u5. The x and z-directions may be seen in Fig. 7a. The associated heat fluxes over the borehole wall vary from 275-375 W/m^2 with a surface mean average value of 310 W/m^2. The differences are evened out quickly and a radial pattern may be seen at a distance of approximately 0.3 m.

The temperature gradient, when heat is injected, will result in an upward flow between the U-pipes and a downward flow at the borehole walls. Between these flows, regions with almost stagnant water will appear; see the blue areas in Fig. 9a. The figure shows the cross-sectional area of the borehole at the vertical level 1.5 m for simulation M_u5. The lengths of the arrows in Fig. 9b indicate the rate of velocity. Towards the ends of the borehole, the speed is decelerated and the transition from inner to outer flow occurs.

In Fig. 10a, temperature differences (ΔT) in the borehole water are shown for different simulations over a line crossing the borehole between the two U-pipe legs in the middle of

the borehole length. The temperature difference is calculated as the difference to the water temperature next to the borehole wall. It may be seen that M_u2 with slightly higher heat transfer rate result in an increased temperature difference. Figure 10b shows the vertical velocities over the same line. All of these simulations have a heat transfer rate of approximately 50 W/m. Due to the non-linearity of the density-temperature curve the lower mean temperature level of the water in M_u2 will result in smaller density differences ($\Delta\rho$), Table 2. Thus, M_u2 has lowest velocities of these three simulations and result in larger borehole thermal resistance.

In Fig. 11a temperature gradient in the borehole water is compared for simulations M_u2 and M_u5 and Fig. 11b shows the associated vertical velocities. Both these simulations have similar water temperatures in the borehole. Simulation M_u5 has twice the heat transfer rate though. The larger heat transfer rate result in an increased temperature gradient in the borehole water. The induced velocities are also higher due to a larger density difference. Notice though that almost the same velocities are achieved in simulations M_u4 (Fig. 10b). That simulation had instead a lower heat transfer rate but a larger mean temperature level. The kinematic viscosity is also lower for M_u4 which result in that the influences between areas with high velocities and almost stagnant water decreases. This indicates that estimation of the borehole thermal resistance should be based on both the mean temperature level in the borehole water and the heat transfer rate.

The Nusselt number may be used to investigate how much the convective heat flow increase the heat transfer rate compared to stagnant water, i.e. with only conductive flow. Figure 12 shows the estimated Nusselt number, Nu* (Eq. 4), as a function of mean borehole water temperature. The thermal resistance in the water for conductive heat flow ($R_{w,c}$) and for total heat transfer (including convective heat flow) ($R_{w,t}$) are calculated from the numerical result (Eq.6). For this geometry the convective flow make the heat transfer approximately 3 times as effective as for stagnant water.

6. Summary and conclusions

In this paper, two different models are presented. An annulus model (M_a) is used in comparison with published results and is shown to be in good agreement with numerical study and experiments for an annulus. A U-pipe model (M_u) was used to investigate the heat transfer in the borehole water and how the convective heat flow influenced the borehole thermal resistance for different heat transfer rates and borehole water temperatures. Surrounding the BHE is solid bedrock with a constant temperature applied at the outer vertical boundary. At the U-pipe outer walls a constant temperature is set.

The U-pipe model was also compared to a laboratory experiment of a three meter long U-pipe borehole. The results show a similar pattern, although lower borehole thermal resistances are achieved in the laboratory experiment. As shown the temperature around the borehole wall differs due to the U-pipe configuration. The achieved difference of 0.35ºC for

simulation M_u5 at the vertical level 1.5 m, will result in a 5% difference in calculated borehole thermal resistance. In the laboratory measurement the temperature were measured at 6 locations at the borehole wall (using 2 measurement points at 3 different levels; top, middle and bottom). A mean value based on six measured values compared to the model value calculated from 9000 cells may fail to incorporate temperature changes around the borehole. Included in the experiment geometry is also the u-pipe bend in the bottom, the plastic pipe representing the borehole wall and an outer boundary of the sand-filled ground region of 0.2 m. Other factors which may influence the result are the assumed pipe conductivity and the calculated thermal resistance in the fluid inside the pipe. There may also have been heat losses from the experimental equipment to the surrounding air. The temperature differences between the borehole wall and the mean fluid temperature in the model are between 0.5 to 0.8ºC higher than the measured temperature difference. In conclusion the model presented in this paper gives good result in comparison with the experiment.

In a groundwater-filled borehole heat exchanger, free convective flow will be induced due to the occurring temperature gradients and the resulting density differences. The convective flow will depend on both the mean temperature level in the groundwater and the heat transfer rate. A high injection rate may give similar borehole thermal resistance result as a lower injection rate if the water temperature is lower for the first case. Therefore, to determine the borehole thermal resistance both heat transfer rate and temperature level must be considered.

The U-pipe configuration result in an un-radial heat transfer pattern close to the borehole. The heat transport will be 2D in the horizontal plane out to a certain radius where a uniform radial heat transport occurs. In simulation M_u5, with a heat flow of 101 W/m, the uniform heat transport is achieved at a radius of about 0.3 m. Borehole heat exchanger system usually operates with heat flows between 10-40 W/m and thermal response test rarely exceeds 100 W/m. It should therefore be possible to restrict numerical models to radius around 1 m if regional groundwater flow not is included. With no regional groundwater flow heat is only distributed by conduction in the bedrock and knowing the undisturbed ground temperature and the thermal influence radius an appropriate outer bedrock boundary temperature (T_{brb}) may be chosen.

By examine the Nusselt number it was determined that the heat transfer approximately increases three times compared to stagnant water in the temperature interval of 10-35ºC. This makes water better than most commercial back-filling materials with regards to heat transfer capacity even though the thermal conductivity is lower for water. However, it should be noted that back-filling, or grouting, may be required when hydraulic sealing of the borehole is necessary or when the ground water level is low.

To disregard the convective flow in heat transfer calculation on groundwater filled borehole heat exchanger result in systems with over capacities. In these simulations giving the same boundary conditions the heat flow was in the range from 33-71 W/m with conductive heat transfer and increased to 47-101 W/m when convective heat flow were included. For a heat injection rate of 50 W/m using only conductive heat transfer result in a temperature

difference between pipe wall and borehole wall of 7.7ºC while using convective heat transfer result in 1.1ºC difference. Thus in system design when considering the heat pumps temperature constraints and the buildings energy demands, calculations with only conductive heat flow will result in a larger required total borehole length.

An ordinary borehole heat exchanger is usually in the order of 50 to 200 meter. There may be other parameters affecting the heat transfer for a longer borehole than for the three meter long investigated in this paper. For example a longer hole will not be influenced of the top and bottom boundary as much as a shorter but the wall boundaries have a larger impact. In [17] result from thermal response tests is compared to simulations from the 3 m long CFD model. They shows similar thermal borehole resistance pattern as been presented in this paper. An ordinary borehole may also interact with connecting fracture which may enlarge the convective flow. It is therefore recommended to perform thermal response test in order to determine the thermal borehole resistance for the specific borehole.

Further studies with this model will be investigations of model approximations such as geometrical approximations and boundary conditions. The goal is to construct a fast, simple model which may be used in TRT analysis and BHE design. It would also be desirable to be able to describe the convective flow when fractures connect to the BHE. Connecting fractures would result in a larger influence area where the convective flow also affects the heat transfer in the bedrock [7]. Since every borehole has an unique set of fractures it is probably preferable to first perform multi-injection rate TRT [18] and combine the result

with a simple and fast design model to determine the convective influence in a water-filled BHE.

References

[1] H. Zeng, N. Diao, Z. Fang, Heat transfer analysis of boreholes in vertical ground heat exchangers, Int. J. of Heat and Mass Transfer 46 (2003) 4467-4481.

[2] C. Yavuzturk, Modeling of vertical ground loop heat exchangers for ground source heat pump systems, Doctoral Thesis, Oklahoma University, USA, 1999.

[3] J. Claesson, G. Hellström, Analytical studies of the influence of regional groundwater flow on the performance of borehole heat exchangers, Terrastock 8th international conference on thermal energy storage, Stuttgart, Germany, 2000.

[4] A. Chiasson, S.J. Rees, J.D. Spitler, A preliminary assessment of the effects of ground-water flow on closed-loop ground-source heat pump systems, ASHRAE Transactions 106(1) (2000) 380-393.

[5] S. Gehlin, G. Hellström, Influence on thermal response test by groundwater flow in vertical fractures in hard rock, Renewable energy 28 (2003) 2221-2238.

[6] H.J.L. Witte, Geothermal response test with heat extraction and heat injection: examples of application in research and design of geothermal heat exchangers, Workshop Lausanne, October 2001.

[7] S. Gehlin, G. Hellström, B. Nordell, The influence of the thermosiphon effect on the thermal response test, Renewable energy 28 (2003) 2239-2254.

[8] Fluent User's guide volume 1-5, Fluent Inc., Centerra Resource Park, Lebanon, USA, 2001.

[9] M. Keyhani, F.A. Kulacki, R.N. Christensen, Free convection in a vertical annulus with constant heat flux on the inner wall, Transactions of the ASME Vol. 105, August, 1983.

[10] D. Littlefield, P. Desai, Buoyant laminar convection in a vertical cylindrical annulus, Transactions of the ASME Vol. 108, November, 1986.

[11] EED – Earth Energy Designer 2.0, Department of physics, Lund University, Lund, Sweden, 2000.

[12] G.S. Kell, E. Whalley, Reanalysis of the density of liquid water in the range of 0-150ºC and 0-1 kbar, the Journal of Chemical Physics, Vol . 62, No. 9, 1975.

[13] F.P. Incropera, D.P. DeWitt, Fundamentals of heat and mass transfer, John Wiley& Sons Inc., Canada, 1996.

[14] G. Hellström, Ground heat storage – Thermal Analyses of duct storage system, theory, PhD thesis, Lund university, Lund, Sweden, 1991.

[15] G. Hellström, Fluid-to-ground thermal resistance in duct ground heat storage, Calorstock'94 6th international conference on thermal energy storage, Espoo, Finland, 1994.

[16] E. Kjellsson, G. Hellström, Laboratory study of the heat transfer in a water-filled borehole with a c-pipe – Preliminary report, Lund University, Lund, Sweden, 1999.

[17] A-M. Gustafsson, S. Gehlin, Influence of natural convection in water-filled boreholes for GCHP, ASHRAE Transaction. NY-08-049, 2008.

[18] Witte H.J.L., van Gelder A.J. (2006), Geothermal response test using controlled multi-power level heating and cooling pulses (MPL-HCP): quantifying ground water effects on heat transport around a borehole heat exchanger, Ecostock 2006, 10th int. conf. on thermal energy storage, The Richard Stockton college of New Jersey, USA.

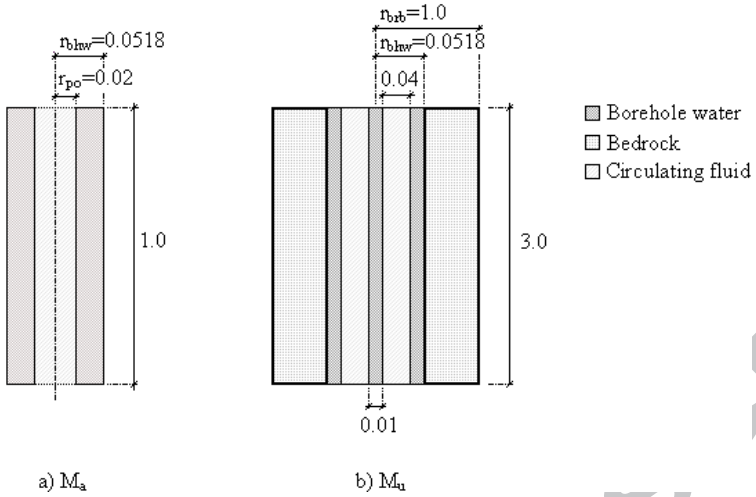

Figure 1. Outline of the model geometries, all dimensions are given in meter.

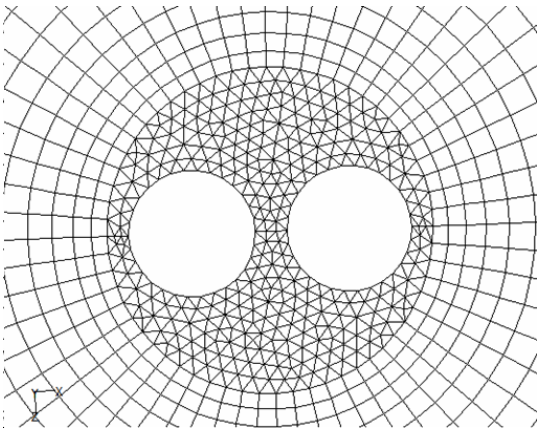

Figure 2. Numerical mesh in a cross-section of the borehole.

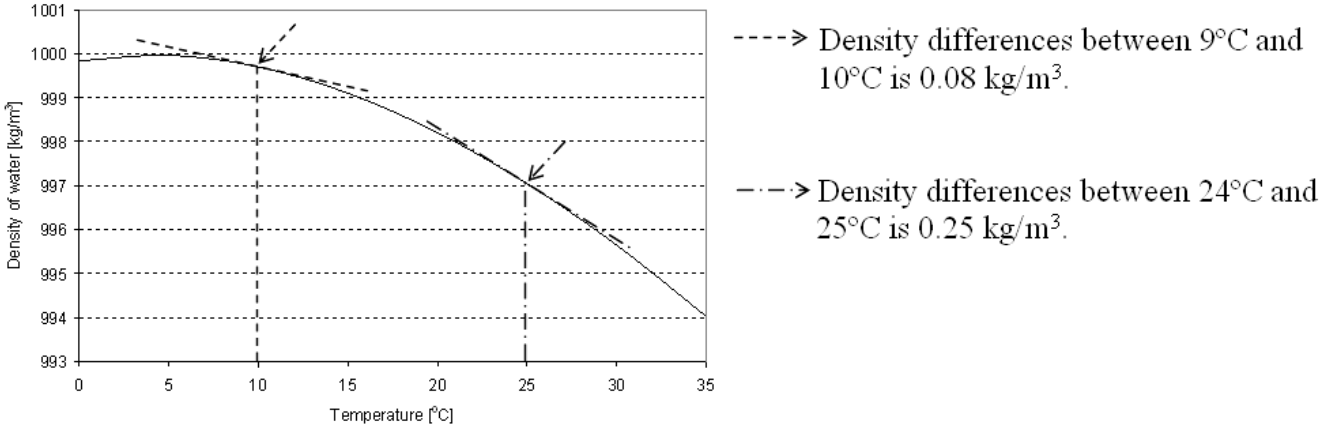

Figure 3: Water density as a function of temperature

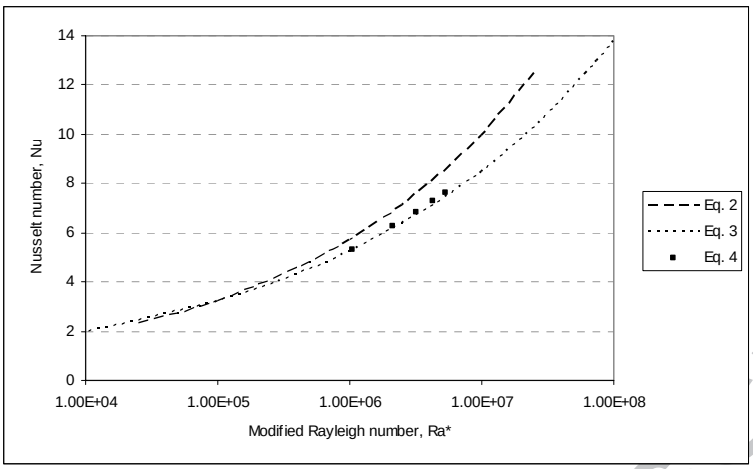

Figure 4. Nusselt number as a function of modified Rayleigh number for Eq. (2), (3) and (4).

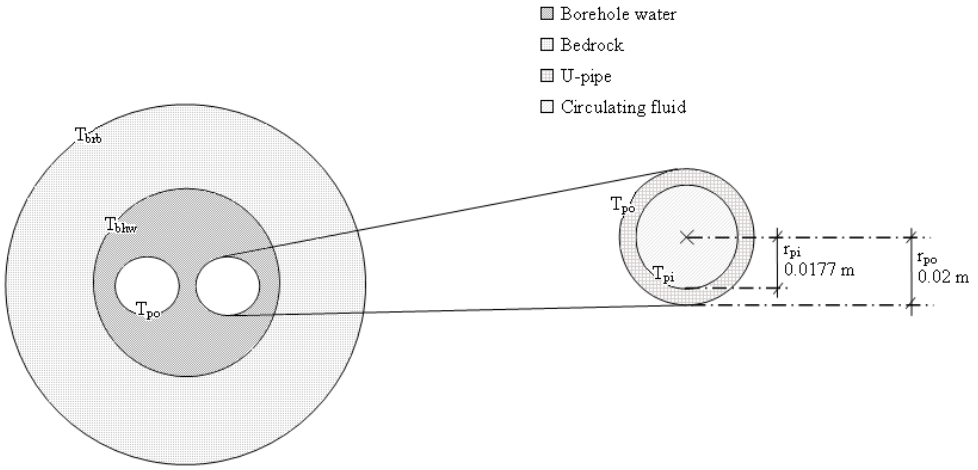

Figure 5. Top view of the U-pipe model, M_u, with additional heat transfer geometry.

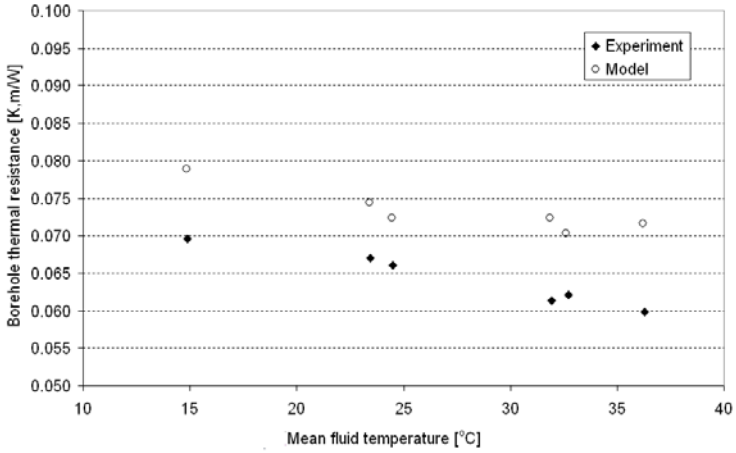

Figure 6. Borehole thermal resistance (R_b) from experiment and model calculations.

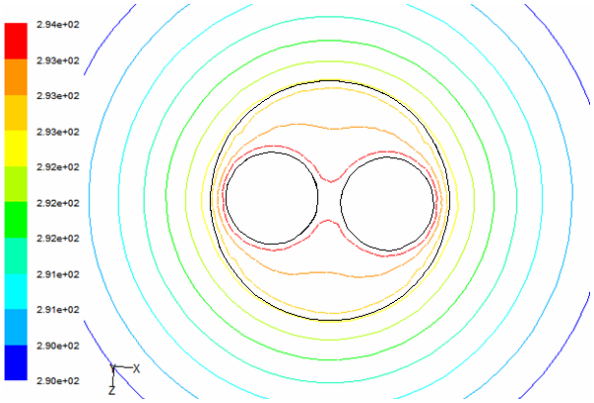

Figure 7.a) Temperatures in and around the borehole for M_u5 at a length of 1.5 m.

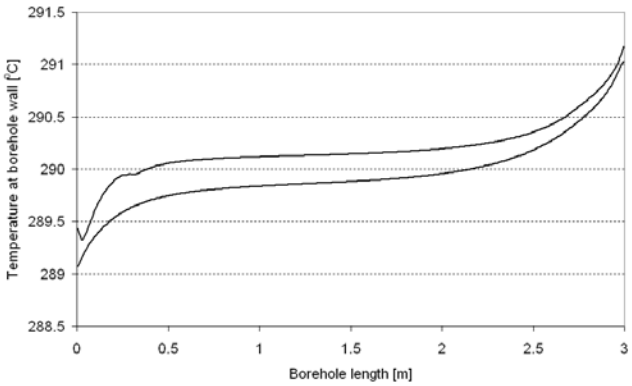

b) Min and max temperatures along the borehole wall in the length direction for M_u5.

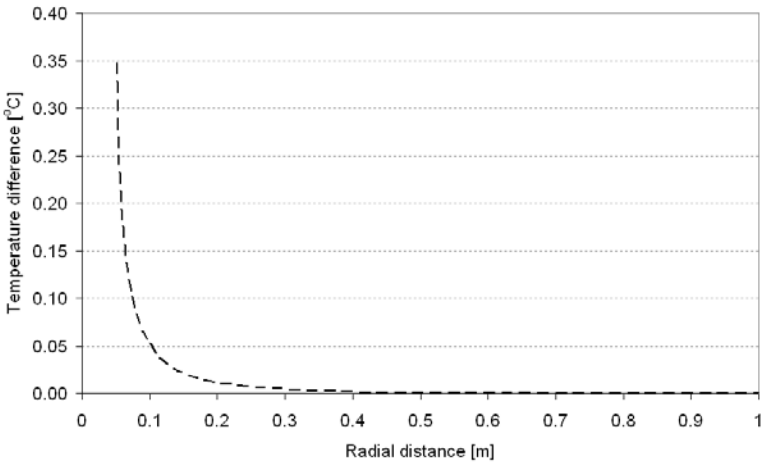

Figure 8. Temperature differences between the x and z direction in the bedrock at vertical level 1.5

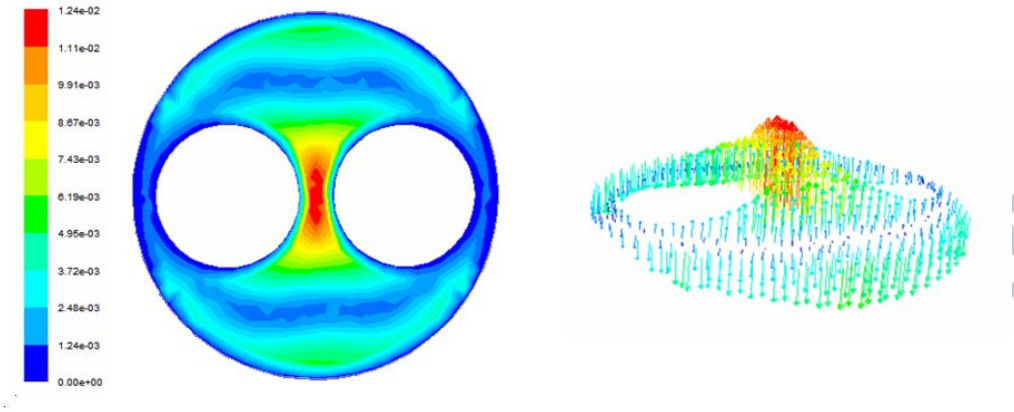

Figure 9.a)Velocity magnitude plot [m/s] *b)velocity vectors for a borehole cross-section*

at the vertical level 1.5 m.

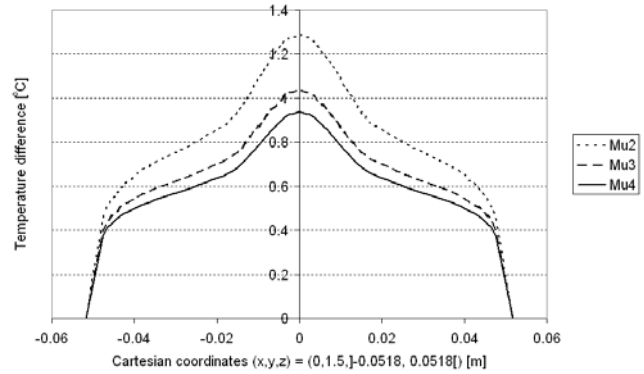

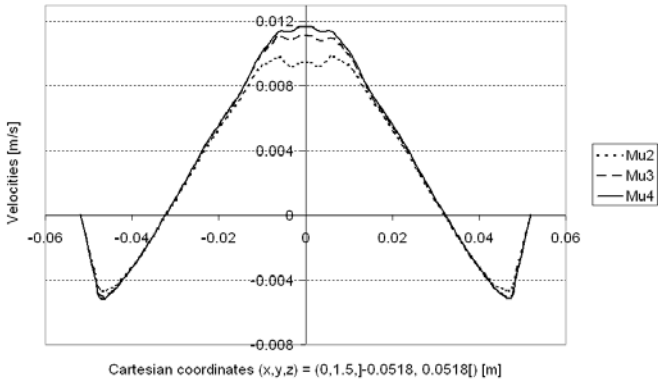

Figure 10.a)Temperature gradient in the borehole b) Velocity profile in the vertical direction for M_u2, M_u3 and M_u4 over a line crossing the middle of the borehole length.

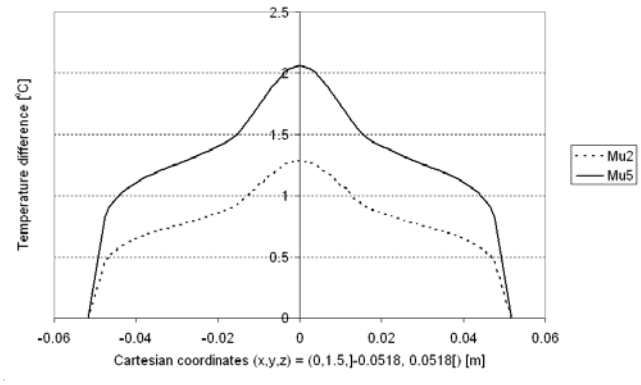

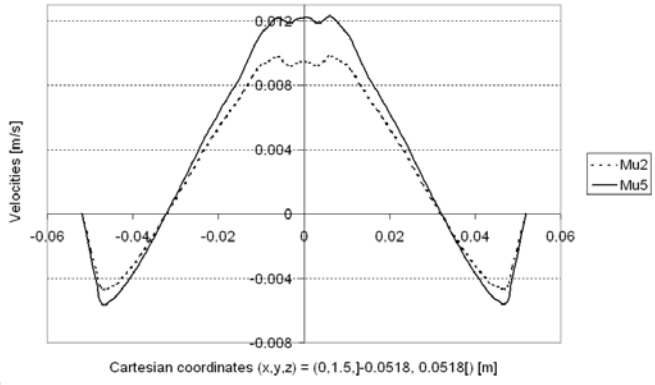

Figure 11a)Temperature gradients in the borehole b)Velocity profiles in the vertical direction for M_u2 and M_u5 over a line crossing the middle of the borehole length.

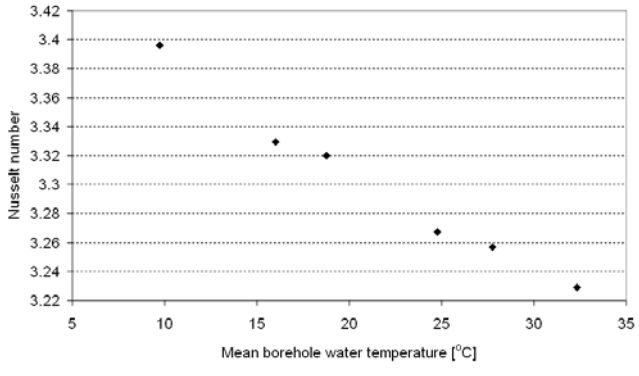

Figure 12. Nusselt number as a function of mean borehole water temperature.

Table 1. Boundary conditions for the laboratory measurement, E1-E12 and boundary conditions and reference parameters for the model calculations, M_u1-M_u6.

Experiment	E1	E2	E3	E4	E5	E6
q' [W/m]	56.89	75.83	95.33	52.22	71.16	90.67
T_{brb} [ºC]	0.79	1.00	1.22	10.64	10.87	10.95

Experiment	E7	E8	E9	E10	E11	E12
q' [W/m]	47.89	65.94	84.77	45.42	64.25	81.84
T_{brb} [ºC]	20.48	20.68	20.79	25.50	25.64	25.79

Model	M_u1	M_u2	M_u3	M_u4	M_u5	M_u6
q' [W/m]	59.49	55.05	49.54	46.74	101.16	95.18
T_{brb} [ºC]	0.79	10.64	20.48	25.51	1.22	10.95
T_{ref} [ºC]	11.43	20.23	28.97	33.45	19.05	27.52
ρ_{ref} [kg/m^3]	999.56	998.16	995.96	994.55	998.39	996.37
β [1/K]	$1.09\cdot10^{-4}$	$2.11\cdot10^{-4}$	$2.95\cdot10^{-4}$	$3.35\cdot10^{-4}$	$1.98\cdot10^{-4}$	$2.82\cdot10^{-4}$
ν [m^2/s]	$1.25\cdot10^{-6}$	$9.95\cdot10^{-7}$	$8.22\cdot10^{-7}$	$7.44\cdot10^{-7}$	$1.02\cdot10^{-6}$	$8.48\cdot10^{-7}$

Table 2: Detailed information for simulations M_u2-M_u5

	M_u2	M_u3	M_u4	M_u5
Mean water temperature [ºC]	20.01	28.87	33.40	18.34
ΔT [ºC]	1.29	1.04	0.94	2.06
$\Delta\rho$ [kg/m^3]	0.26	0.30	0.31	0.38
Max velocities [m/s]	$9.92 \cdot 10^{-3}$	$1.24 \cdot 10^{-2}$	$1.17 \cdot 10^{-2}$	$1.24 \cdot 10^{-2}$
R_b [m,K/W]	0.077	0.074	0.073	0.075